Polymer Journal, Vol. 35, No. 7, pp 560—567 (2003)

Energy Absorption in Chopped Carbon Fiber Epoxy Composites for Automotive Crashworthiness

George Chennakattu JACOB,† James Michael STARBUCK,* John Francis FELLERS,** and Srdan SIMUNOVIC***

Materials Science and Engineering Department, University of Tennessee, Knoxville, 434 Dougherty Engineering, Knoxville, TN 37996, USA
**Polymer Matrix Composites Group, Metals and Ceramics Division, Oak Ridge National Laboratory, Post Office Box 2009, Oak Ridge, TN 37831–8048, USA*
***Materials Science and Engineering Department, University of Tennessee, Knoxville, 608 Dougherty Engineering, Knoxville, TN 37996, USA*
****Computational Material Science, Computer Science and Mathematics Division, Oak Ridge National Laboratory, Post Office Box 2008, Bldg. 6025, MS–6359, Oak Ridge, TN 37831–6359, USA*

(Received December 24, 2002; Accepted May 13, 2003)

ABSTRACT: In the crashworthiness of automotive structures, the primary issues to the automotive industry are the overall economy and the weight of the material. To reduce the weight and improve the fuel economy, polymer composite materials have replaced more and more metal parts in vehicles. They have the added benefit of being able to dissipate large amounts of impact energy by progressive crushing. To identify and quantify the energy absorbing mechanisms in candidate automotive composite materials, test methodologies were developed for conducting progressive crush tests on composite plate specimens. The test method development and experimental set-up focused on isolating the damage modes associated with the frond formation that occurs in dynamic testing of composite tubes. Quasi-static progressive crush tests were performed to quantify the effects of specimen width, profile radius and profile constraint on the specific energy absorption and failure modes of composite plates manufactured from chopped carbon fiber (CCF) with an epoxy resin system using compression molding techniques. The carbon fiber was Toray T700 and the epoxy resin was YLA RS-35. It was demonstrated during testing that the use of a roller constraint directed the crushing process and the load deflection curves were similar to the progressive crushing of tubes. Modifications to the basic specimen geometry were required when testing material systems that have low axial stiffness to prevent a global buckling mode. The experimental data in conjunction with the test observations were used to develop analytical models for predicting the crashworthiness of automotive composite structures.

KEY WORDS Crashworthiness / Energy Absorption / Composite Materials / Crush Testing / Plates / Chopped Fiber / Carbon Epoxy /

In passenger vehicles the ability to absorb impact energy and be survivable for the occupant is called the "crash worthiness" of the structure. This absorption of energy is through controlled failure mechanisms and modes that enable the maintenance of a gradual decay in the load profile. The crashworthiness of a material is expressed in terms of its specific energy absorption (SEA) which is characteristic to that particular material. It is defined as the energy absorbed per unit mass of crushed material. Mathematically $SEA = W/(V\rho)$, where the total energy absorbed, W, is calculated by integrating the area under the load-deflection curve, V is the volume of crushed material, and ρ is the density of the material.

Vehicle size and mass provide a certain degree of protection but can have negative inertial effects. Driven by the need to overcome these negative effects of both size and mass coupled with mandates for increased fuel efficiency, an attempt is being made to use composites in the development of energy dissipating devices. The ability to tailor composites, in addition to their attributes of high stiffness-to-weight and strength-to-weight ratios, fatigue resistance and corrosion resistance, makes them very attractive in crashworthiness. The challenge is the use of specific features of geometry and materials in enabling greater safety while simultaneously decreasing the weight, without negatively affecting the overall economics of fabrication and production.

To reduce the overall weight and improve the fuel economy of vehicles, more and more metal parts are being replaced by polymer composite materials. Contrary to metals, especially in compression, most composites are generally characterized by a brittle rather than ductile response to load. While metal structures collapse under crush or impact by buckling and/or folding in accordion (concertina) type fashion involving extensive plastic deformation, composites fail through a sequence

†To whom correspondence should be addressed (Phone: +1-865-946-1295, Fax: +1-865-574-8257, E-mail: gjacob@utk.edu).

of fracture mechanisms involving fiber fracture, matrix crazing and cracking, fiber-matrix de-bonding, delamination, and inter-ply separation. The actual mechanisms and sequence of damage are highly dependent on the geometry of the structure, lamina orientation, type of trigger, and crush speed, all of which can be suitably designed to develop high energy absorbing mechanisms.

Much of the experimental work to study the effects of fiber type, matrix type, fiber architecture, specimen geometry, testing speed, fiber volume fraction, and processing conditions on the energy absorption of composite materials has been carried out on axisymmetric tubes.[1–44] Tube structures are relatively easy to fabricate and close to the geometry of the actual crashworthy structures. These tubes were designed to absorb impact energy in a controlled manner by providing a trigger to initiate progressive crushing.

In the progressive crushing of composite tubes there are many different failure mechanisms that contribute to the overall energy absorption of the structure. To isolate the damage mechanisms and quantify the energy absorption in chopped carbon fiber composites, the CCF plate specimens were tested using a unique test fixture.

EXPERIMENTAL

Material System Investigated. Chopped Carbon Fiber/ Epoxy Resin System

Composite materials are recognized as being efficient energy absorbers, however for a material to be suitable for automotive crashworthy structural applications they must also have low raw material and manufacturing costs. The use of chopped carbon fiber and compression molded processing methods has the potential to satisfy these criteria. Hence the ACC (automotive composite consortium) was interested in investigating the use of carbon fibers in chopped fiber reinforced composite materials. Carbon fiber reinforced tubes display higher specific energy absorption than other fiber-reinforced tubes. This is a direct result of the lower density of the carbon fiber thus also contributing to the lightweight of the structures they are used in. Epoxy, which is regarded as a standard resin that frequently finds use in most composites was chosen as the matrix.

The chopped carbon fiber composites were fabricated using Toray T700 carbon fiber with YLA RS-35 epoxy resin. YLA supplied the molding compound and CCS compression molded the plates. Below is the detailed procedure that was employed to make the chopped carbon fiber panels for testing.

Making of the Molding Compound.

1. Fiber: Upwards of 200 creels of fiber was loaded into the feed rack on the prepreg machine.
2. Resin: On a separate machine, the resin system was mixed and transformed into a film of uniform thickness.
3. Prepreg: The fiber tows were spread to a very accurate FAW (fiber aerial weight defined as the weight per unit area of the fiber) and then mated with the resin film.
4. Prepreg: The impregnated fibers were then rolled up at the end of the line.
5. Molding Compound: After a few days (these days are given for some chemical reaction to complete) the prepreg was then slit and chopped to a specified width and length.
6. Stock: The material was then freezer stored while it awaited a molding requirement.

Part Molding.

7. Tooling: A master mold base was loaded into a press. A core and cavity die set was installed onto the master base. The ejector system was installed into the assembly. The heating and temperature controls were also installed into the assembly. The system was heated up and a shear edge check was performed. Finally, the tool was released, and was ready to go.
8. Charge Prep: The material charge was weighed and placed into the preheat mold.
9. Preheat: The material was preheated at 150 °F in an oven for 30 min.
10. Load Tool: The material was then pulled from the preheat tool and placed into the molding tool. The tool was rapidly closed to a “trigger point”, where the low pressure pump transitions to the high pressure pump.
11. Pressing the Part: The process cycle then involved applying “pinch” pressure onto the material for a fixed condition of about 100 psi, for 15 to 60 s. The process then was automatically switched to full pressure for the full cure cycle. This was at a molding pressure of 2000 psi, for 30 min, at a temperature of 295 °F.
12. Ejection: The part was then ejected with a 5 point ejection system, and it was then placed in a cool down clamp fixture for about 10 min.
13. The edges were then deflashed and the post weight was recorded in the logbook.

Test Method

A new test fixture design was developed for determining the deformation behavior and damage mechanisms that occur during progressive crushing of com-

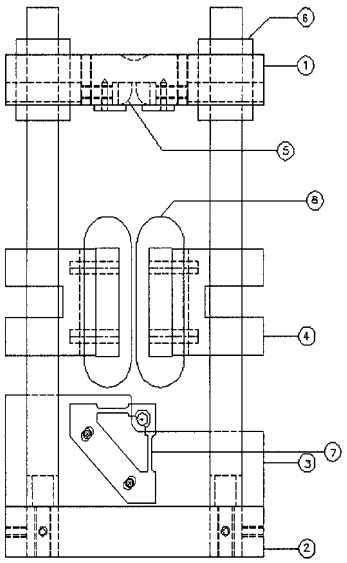

Figure 1. Schematic of test fixture design.

posite materials. The fixture was designed to isolate damage modes associated with frond formation (splaying mode) in composite tubes by testing plate geometries. The design of the test fixture can accommodate different plate widths (up to a maximum of 50 mm), plate thicknesses (3 mm ± 1.5 mm), contact profile shapes (profile block radius: 6.4 mm and 13 mm), and contact profile constraints (tight, loose, and no constraint). A schematic of the test fixture is shown in Figure 1 and photos are shown in Figures 2 and 3. Features incorporated into the design include an observable crush zone, long crush length (50 mm), interchangeable contact profile, frictionless roller for contact constraint, and out of plane roller supports to prevent buckling. Below is a list of the primary components of the fixture (please see Figure 1).

1. Top plate
2. Base plate
3. Profile block
4. Roller plate
5. Grip plate and insert
6. Linear shaft and bearing
7. Load cell
8. Roller way

The brackets on each side of the profile plate were designed to provide a method of constraining the specimen to deform along the path of the contact profile. The severity of the contact profile constraint was determined by the position of the brackets and was adjustable using slotted positioning holes. The objective of the profile constraint was to determine if different damage mechanisms could be activated depending on the position of the roller. Figure 4 depicts the different constraint conditions. Starbuck *et al.*[45] provides more details of the fixture design.

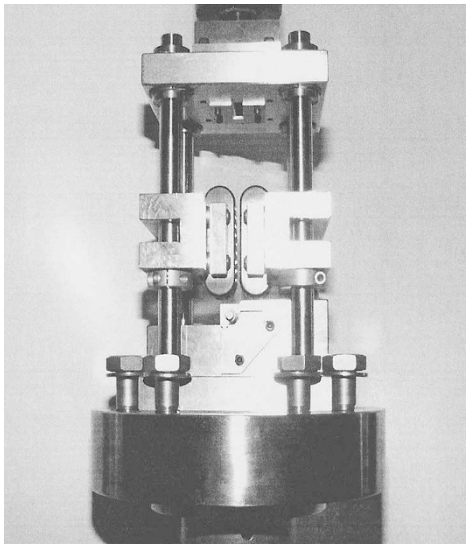

Figure 2. Test fixture assembly.

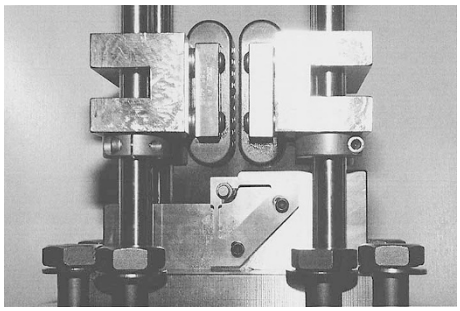

Figure 3. Roller ways and contact profile constraint.

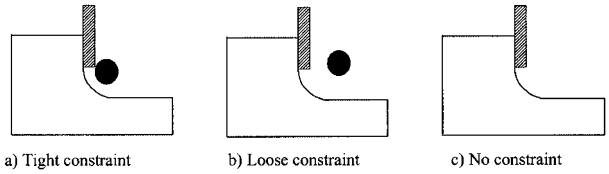

Figure 4. Constraint conditions.

Practical considerations related to the cost of production of the test specimens were of paramount importance in developing the test methodology. Composite plate specimens are very cheap to fabricate and it has been observed that plate specimens progressively crush in modes very similar to the damage modes that occur during progressive crushing of composite tubes. Also plates can be easily produced with consistently high quality. The CCF specimen plates had a nominal length of 178 mm (7 inches) and a width of 50 mm (2 inches), 25.4 mm (1 inch) or 13 mm (0.5 inches) and a 45° chamfer was used as the crush initiator. The specimen configuration is shown in Figure 5. A diamond cut off wheel was used to cut the specimens off the composite panel. No coolant was used during cutting to prevent contamination of the test specimens. A servo-hydraulic test machine and a loading rate of 5 mm min^{-1} (0.2 inches min^{-1}) were used through out

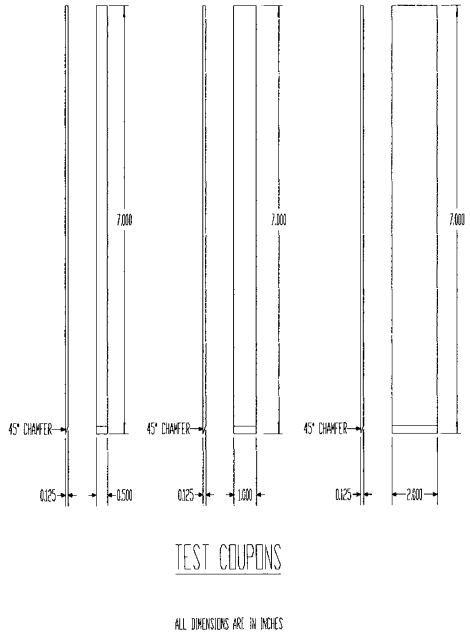

Figure 5. Specimen configuration.

the entire testing. The load-deflection response was recorded using a computerized data acquisition system. The area under the load deflection curve was calculated for the total energy absorbed and the initial peak load and sustained crush load were identified.

Variables Investigated

Eight panel groups of compression molded chopped carbon fiber/epoxy composites having different material properties were made. Descriptions of the various panel groups are given below.

1. Panel Group Name: CCF1
   Fiber Tow Size: 150 gsm (12 K)
   Fiber Volume Fraction: 40%
   Fiber Length: 1 inch
2. Panel Group Name: CCF2
   Fiber Tow Size: 150 gsm (12 K)
   Fiber Volume Fraction: 40%
   Fiber Length: 2 inches
3. Panel Group Name: CCF3
   Fiber Tow Size: 300 gsm (48 K)
   Fiber Volume Fraction: 40%
   Fiber Length: 2 inches
4. Panel Group Name: CCF5
   Fiber Tow Size: 150 gsm (12 K)
   Fiber Volume Fraction: 50%
   Fiber Length: 1 inch
5. Panel Group Name: CCF6
   Fiber Tow Size: 150 gsm (12 K)
   Fiber Volume Fraction: 50%
   Fiber Length: 2 inches
6. Panel Group Name: CCF7
   Fiber Tow Size: 300 gsm (48 K)
   Fiber Volume Fraction: 50%
   Fiber Length: 2 inches
7. Panel Group Name: CCF8
   Fiber Tow Size: 300 gsm (48 K)
   Fiber Volume Fraction: 40%
   Fiber Length: 1 inch
8. Panel Group Name: CCF9
   Fiber Tow Size: 300 gsm (48 K)
   Fiber Volume Fraction: 50%
   Fiber Length: 1 inch

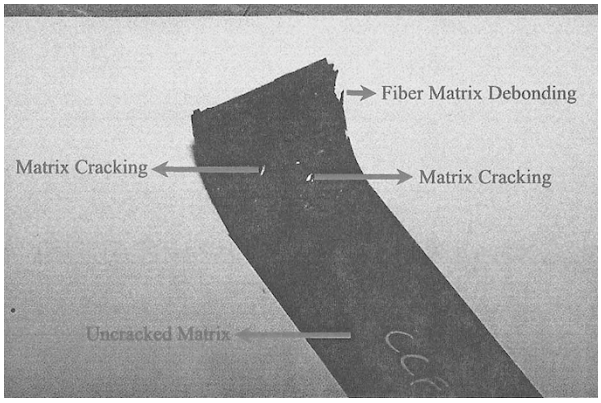

Figure 6. Crushed CCF specimen.

Quasi-static progressive crush tests (3 replicates at each condition) were performed to study the effects of specimen width, profile radius and profile constraint on the energy absorption characteristics of the above panel groups. Below is a summary of the various test variables that were investigated.

- Profile Radius: 6.4 mm (0.25 inches), 13 mm (0.5 inches)
- Constraint: None, Loose, Tight
- Plate Width: 13 mm (0.5 inches), 25.4 mm (1 inch), 50 mm (2 inches)

RESULTS AND DISCUSSION

For all specimens tested, local crushing took place at the chamfered end of the plates. Matrix cracking occurred at the ends of the fiber tows due to stress concentration at these ends. Fiber-matrix debonding also took place in a majority of the specimens that were tested. Figure 6 depicts a crushed CCF specimen having matrix cracks and fiber matrix debonding. Flexural deformations controlled the damage process. Some of the test specimens when loaded in the no constraint condition experienced fiber pull out, fiber breakage in the tension side and fiber buckling in the compression side of the specimen. The fracture mechanism that took place in specimens crushed in the loose and tight constraint condition were the same in all of the specimens and the specimen failure was more or less predictable.

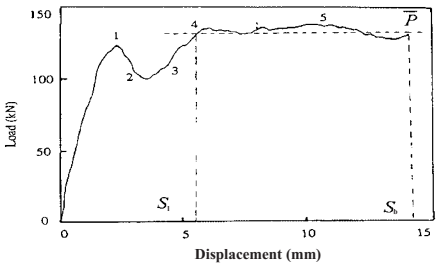

Figure 7. Typical load displacement curve for a progressively crushed composite tube.[34]

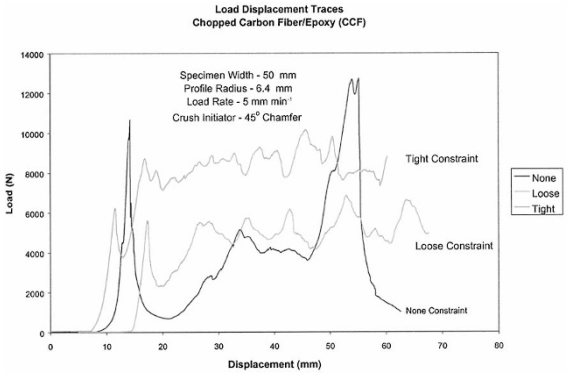

Figure 8. Load displacement traces for CCF.

On the contrary the specimens that were crushed in the no constraint condition fractured in rather erratic fashions and specimen failure was far less predictable. This was due to absence of the much needed roller constraint required to direct the crushing process. Some of the no constraint tests lead to catastrophic failure of the specimen where in the specimen broke in to 2 or 3 pieces.

Figure 7[34] is a typical load displacement curve obtained from progressive crushing of a composite tube specimen. Please see Figure 8 for the load displacement traces recorded for a CCF composite material. It can be noted by comparing Figures 7 and 8 that the CCF specimens tested in the loose and tight constraint conditions generated load deflection curves that were similar to the ones generated during the progressive crushing of composite tubes. It had 4 stages, the first one being characterized by an initial rapid load increase. A rapid load drop occurred in the second stage of the load deflection curve followed by a gradual saturation of the load. The final stage was characterized by stable crushing at a constant mean load. The small load fluctuations and serrations in the fourth stage of the curve are characteristic of stable crushing.

Effect of Profile Radius

In all the tests performed on chopped carbon fiber composite materials, irrespective of the specimen width or the constraint condition, an increase in the profile radius caused a decrease in the specific energy absorption, SEA. For a comparison of the load displacement

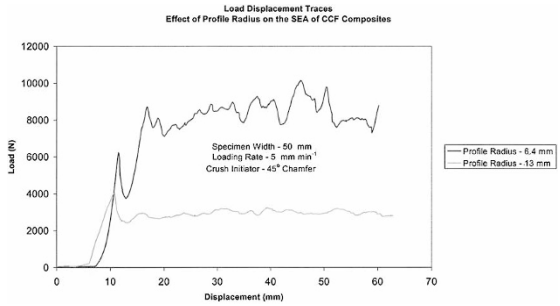

Figure 9. Load displacement traces representing the effect of profile radius on the SEA of CCF.

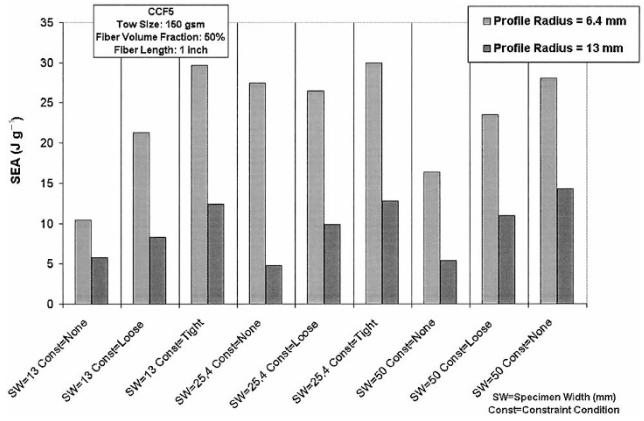

Figure 10. Variation of SEA with profile radius for CCF.

traces recorded for a test conducted on a specimen using a profile bock of radius 6.4 mm and on a specimen using a profile block of radius 13 mm please see Figure 9.

The decrease in SEA with an increase in the profile radius is due to the fact that a specimen loaded in compression is crushed through the contact profile as defined by the profile block. When a larger radius is used the specimen follows a smoother curve that requires less axial load to produce the flexural deformations. Therefore, less energy is absorbed during the progressive crush test. Please see Figure 10.

Effect of Specimen Width

The test fixture design can accommodate plate specimen widths up to a maximum of 50 mm (2 inches). An understanding of how energy absorption is affected by changes in specimen width can in the long run reduce costs by allowing the favorable use of smaller structures for automotive crashworthiness. In all the tests conducted irrespective of the constraint condition or the radius of the profile block, the 50 mm (2 inches) wide specimens displayed the highest specific energy absorption. Either the 25.4 mm (1 inch) or the 13 mm (0.5 inches) wide specimens followed it. For a comparison of the load displacement traces recorded for a test conducted on a specimen of width 13 mm (0.5 inches),

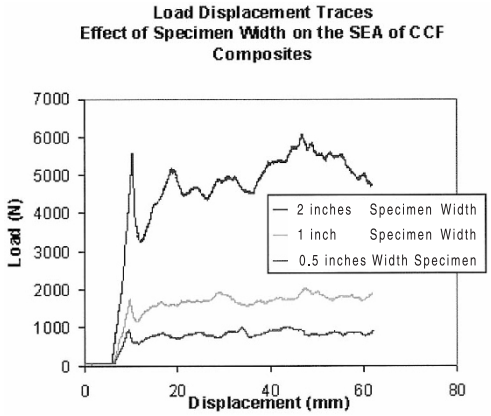

Figure 11. Load displacement traces representing the effect of specimen width on the SEA of CCF.

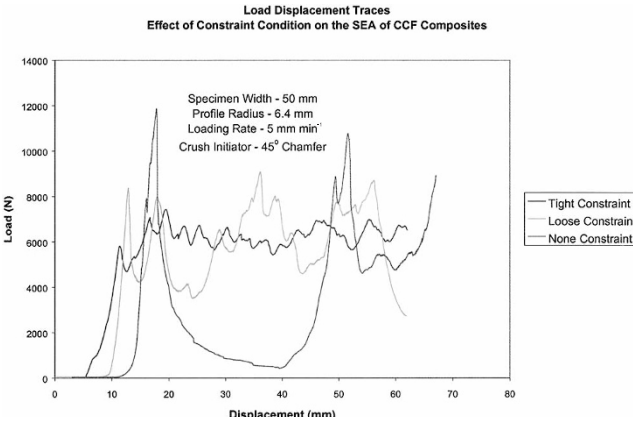

Figure 13. Load displacement traces representing the effect of constraint condition on the SEA of CCF.

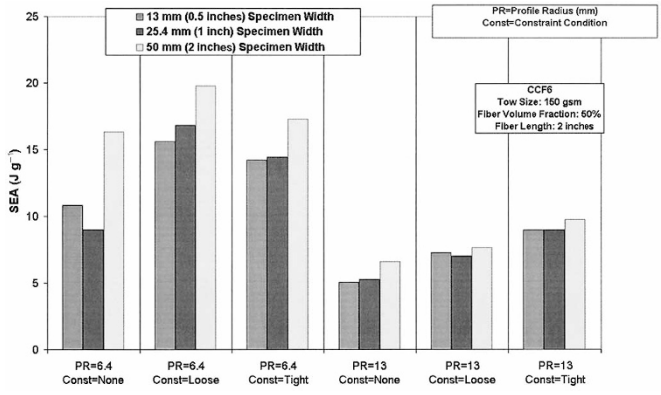

Figure 12. Variation of SEA with specimen width for CCF.

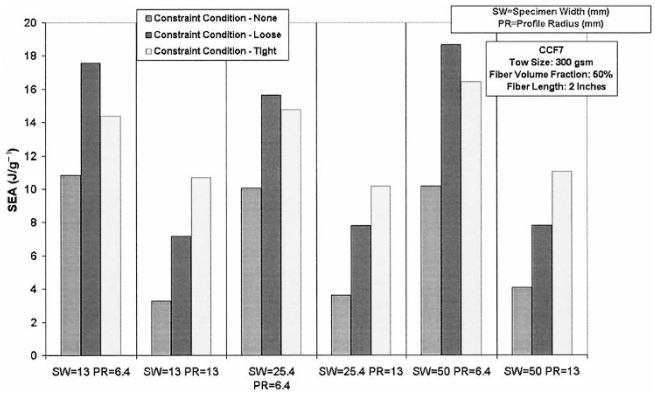

Figure 14. Variation of SEA with constraint condition for CCF.

25.4 mm (1 inch), and 50 mm (2 inches) respectively please see Figure 11.

The reason for the superior energy absorption in the 50 mm (2 inches) wide specimens was due to the fact that the fibers in them had fiber lengths less than or equal to the width of the specimen unlike the case of the 13 mm (0.5 inches) and the 25.4 mm (1 inch) wide specimens that had fibers with fiber lengths greater than the width of the specimen. This results in fewer fiber ends for the narrower specimens and consequently fewer fracture initiation sites. Please see Figure 12.

Effect of Constraint

The tests conducted on the CCF material were only successful when the roller was positioned in the tight and loose constraint condition. When the no constraint condition was attempted the initial peak load increased and the CCF specimens buckled between the top plate and roller ways. The roller ways were unsuccessful in preventing out-of-plane buckling in the CCF material because of its low buckling strength. This resulted in having to use a metal push plate to reduce the unsupported specimen length. The metal plate was 76 mm in length and was bonded to the end of the CCF specimens using 5 min epoxy. This specimen configuration was successful when the roller was positioned in the no constraint condition.

The no constraint condition resulted in the highest initial peak load relative to the other constraint conditions.

Comparing the SEA's, the lowest SEA corresponded to the no constraint condition when compared to either tight or loose constraint condition. For a comparison of the load displacement traces recorded for a test conducted on a specimen in the no constraint, the loose constraint and the tight constraint condition respectively please see Figure 13. Please see Figure 14.

CONCLUSION

Quasi-static progressive crush strip tests were conducted on randomly oriented CCF composite materials to evaluate their energy absorption capability. The objective of the test method was to simulate the frond formation observed during dynamic crush tests of composite tubes. The test program considered three test parameters: specimen width, profile radius, and profile constraint. The experimental data in conjunction with the test observations were used to develop analyt-

ical models for predicting the crashworthiness of automotive composite structures. It was demonstrated during testing that different damage mechanisms could be activated depending on the condition of the profile constraint. The use of a roller constraint directed the crushing process and the load deflection curves were similar to progressive crushing of tubes. Modifications to the basic specimen geometry were required when testing the CCF material systems that have a low axial stiffness. For example, the tests conducted on the CCF material were not successful when the roller was positioned in the no constraint condition. In the no constraint condition the initial peak load increased and the specimen buckled between the top plate and roller ways. The roller ways were unsuccessful in preventing out-of-plane buckling in the CCF material because of its low buckling strength. This resulted in having to use a 76 mm long metal push plate to reduce the unsupported specimen length. In all the tests conducted, irrespective of the constraint condition or the radius of the profile block used, the 2 inches wide specimens displayed the highest specific energy absorption, SEA, when compared to that of the 0.5 inches and 1 inch wide specimens. An increase in the radius of the profile block caused a decrease in the specific energy absorption, SEA. The no constraint condition resulted in the highest initial peak load and the lowest specific energy absorption, SEA, relative to the other constraint conditions.

Acknowledgment. Research was sponsored by the U.S. Department of Energy, Assistant Secretary for Energy Efficiency and Renewable Energy, Office of Transportation Technologies, Lightweight Materials Program, under contract DE-AC05-00OR22725 with UT-Battelle, LLC.

REFERENCES

1. D. Hull, *Compos. Sci. Technol.*, **40**, 377 (1991).
2. G. L. Farley, "Energy Absorption of Composite Material and Structures", Proc. 43rd American Helicopter Society Annual Forum, St. Louis, MO, 1987, pp 613–627.
3. G. L. Farley, *J. Compos. Mater.*, **20**, 390 (1986).
4. G. L. Farley, *J. Compos. Mater.*, **17**, 267 (1983).
5. G. L. Farley, *J. Compos. Mater.*, **20**, 322 (1986).
6. G. L. Farley, in "Energy Absorption in Composite Materials for Crashworthy Structures", Proc. of ICCM 6, F. L. Matthews, N. C. R. Buskell, J. M. Hodgkinson, and J. Mortan, Eds., Elsevier Science Publishers Limited, London, 1987, pp 3.57–3.66.
7. P. H. Thornton and P. J. Edwards, *J. Compos. Mater.*, **16**, 521 (1982).
8. D. Hull, 'Axial Crushing of Fibre Reinforced Composite Tubes' in "Structural Crashworthiness", N. Jones and T. Weirzbicki, Eds., Butterworths, London, 1983, pp 118–135.
9. H. Hamada, S. Ramakrishna, Z. Maekawa, and M. Nakamura, Proc. 10th Annual ASM/ESD Advanced Composite Conference, Dearborn, MI, November 7–10, 1994, pp 511–522.
10. D. W. Schmuesser and L. E. Wickliffe, *J. Eng. Mat. & Tech.*, **109**, 72 (1987).
11. H. Hamada and S. Ramakrishna, *J. Thermoplast. Compos. Mater.*, **9**, 259 (1996).
12. G. L. Farley and R. M. Jones, *J. Compos. Mater.*, **26**, 78 (1992).
13. G. L. Farley, *J. Compos. Mater.*, **26**, 388 (1992).
14. P. H. Thornton, *J. Compos. Mater.*, **13**, 247 (1979).
15. C. H. Chiu, C. K. Lu, and C. M. Wu, *J. Compos. Mater.*, **31**, 2309 (1997).
16. C. H. Chiu, C. K. Lu, and C. M. Wu, 'Energy Absorption of Three-Dimensional Braided Composite Tubes', in "Proc. of ICCM 10", B. C. Whistler, Ed., Woodhead Publishing Limited, 1995, pp 4.187–4.194.
17. S. Ramakrishna, H. Hamada, Z. Maekawa, and H. Sato, *J. Thermoplast. Compos. Mater.*, **8**, 323 (1995).
18. I. Y. Chang and J. K. Lees, *J. Thermoplast. Compos. Mater.*, **1**, 277 (1988).
19. I. Y. Chang, *Compos. Sci. Technol.*, **24**, 61 (1985).
20. H. Satoh, H. Hirakawa, Z. Maekawa, H. Hamada, M. Nakamura, and D. Hull, 38th International SAMPE Symposium, Science of Advanced Materials and Process Engineering Series, vol. 38, Anaheim, CA, May 10–13, 1993, pp 952–966.
21. H. Hamada, J. C. Coppola, D. Hull, Z. Maekawa, H. Sato, *Composites*, **23**, 245 (1992).
22. G. L. Farley and R. M. Jones, "Energy Absorption Capability of Composite Tubes and Beams", NASA TM-101634, AVSCOM TR-89-B-003, (1989).
23. D. Hull, 'Energy Absorption of Composite Materials Under Crash Conditions' in "Proc. of ICCM 4", T. Hayashi, K. Kawata, and S. Umekawa, Eds., Japan Society for Composite Materials, Tokyo, 1982, pp 861–870.
24. J. P. Berry, Ph. D. Thesis in Metallurgy, University of Liverpool, 1984.
25. G. L. Farley, "Crash Energy Absorbing Composite Sub-floor Structure", 27th SDM conference, San Antonio, TX, (May 1986). Also submitted for publication to The American Helicopter Society.
26. G. L. Farley and R. M. Jones, *J. Compos. Mater.*, **26**, 1741 (1992).
27. P. H. Thornton, J. J. Harwood, and P. Beardmore, *Compos. Sci. Technol.*, **24**, 275 (1985).
28. D. D. Dubey, J. A. Vizzini, *J. Compos. Mater.*, **32**, 158 (1998).
29. H. Hamada, S. Ramakrishna, Z. Maekawa, M. Nakamura, and T. Nishiwaki, Proc. 10th Annual ASM/ESD Advanced Composite Conference, Dearborn, MI., November 7–10, 1994, pp 523–534.
30. A. G. Mamalis, Y. B. Yuan, and G. L. Viegelahn, *Int. J. Veh. Des.*, **13(5/6)**, 564 (1992).
31. A. H. Fairfull, Ph. D. Thesis in Materials Science, University of Liverpool, 1986.
32. A. H. Fairfull and D. Hull, 'Effects of Specimen Dimensions on the Specific Energy Absorption of Fibre Composite Tubes' in "Proc. of ICCM 6", F. L. Matthews, N. C. R. Buskell, J.

M. Hodgkinson, J. Morton, Eds., Elsevier Science Publishers Limited, London, 1987, pp 3.36–3.45.
33. G. L. Farley, 'Energy Absorption Capability and Scalability of Square Cross Section Composite Tube Specimens', in "U.S. Army Research and Technology Activity–AVSCOM", NASA-TM 89087, 1989, pp 1–17.
34. S. Ramakrishna and H. Hamada, *Key Eng. Mat.*, **141**–**143**, 585 (1998).
35. S. Hanagud, J. I. Craig, P. Sriram, and W. Zhou, *J. Compos. Mater.*, **23**, 448 (1989).
36. H. Hamada, S. Ramakrishna, Z. Maekawa, and H. Sato, *J. Poly. & Poly. Comp.*, **3**, 99 (1995).
37. S. Ramakrishna and D. Hull, *Compos. Sci. Technol.*, **49**, 349 (1993).
38. S. Ramakrishna, *J. Reinf. Plast. Comp.*, **14**, 1121 (1995).
39. P. Snowdon and D. Hull, Proc. Fiber Reinforced Composites Conference'84, Plastics and Rubber Institute, April 3–5, 1984, pp 5.1–5.10.
40. P. H. Thornton, W. H. Tao, and R. E. Robertson, Advanced Composite Materials: New Development and Applications Conference Proceedings, Detroit, MI., September 30–October 3, 1991, pp 489–496.
41. D. C. Bannerman and C. M. Kindervater, Proc. 4th International SAMPE European Chapter, Bordeaux, 1984, pp 155–167.
42. P. H. Thornton, *J. Compos. Mater.*, **24**, 594 (1990).
43. G. L. Farley, *J. Compos. Mater.*, **25**, 1314 (1991).
44. C. M. Kindervater, Presented at Natuional Specialists Meeting, Composite Structures of the American Helicopter Society, Philadelphia, P. A., March 23–25, 1983.
45. J. M. Starbuck, G. C. Jacob, and S. Simunovic, Presented at Future Car Congress, Crystal City, VA, April 2–6, 2000.